2013-06-15

JNK regulates compliance-induced adherens junctions formation in epithelial cells and tissues

Hui You
State University of New York at Buffalo

Et al.

JNK regulates compliance-induced adherens junctions formation in epithelial cells and tissues

Hui You[1], Roshan M. Padmashali[1], Aishwarya Ranganathan[1], Pedro Lei[1], Nomeda Girnius[2], Roger J. Davis[2] and Stelios T. Andreadis[1,3,4,*]

[1]Bioengineering Laboratory, Department of Chemical and Biological Engineering, University at Buffalo, the State University of New York, Amherst, NY 14260, USA
[2]Howard Hughes Medical Institute and Program in Molecular Medicine, University of Massachusetts Medical School, Worcester, MA 01605, USA
[3]Department of Biomedical Engineering, University at Buffalo, the State University of New York, Amherst, NY 14260, USA
[4]Center for Excellence in Bioinformatics and Life Sciences, University at Buffalo, the State University of New York, Amherst, NY 14260, USA
*Author for correspondence (sandread@buffalo.edu)

Accepted 12 March 2013
Journal of Cell Science 126, 2718–2729

doi: 10.1242/jcs.122903

Summary

We demonstrate that c-Jun N-terminal kinase (JNK) responds to substrate stiffness and regulates adherens junction (AJ) formation in epithelial cells in 2D cultures and in 3D tissues *in vitro* and *in vivo*. Rigid substrates led to JNK activation and AJ disassembly, whereas soft matrices suppressed JNK activity leading to AJ formation. Expression of constitutively active JNK (MKK7-JNK1) induced AJ dissolution even on soft substrates, whereas JNK knockdown (using shJNK) induced AJ formation even on hard substrates. In human epidermis, basal cells expressed phosphorylated JNK but lacked AJ, whereas suprabasal keratinocytes contained strong AJ but lacked phosphorylated JNK. AJ formation was significantly impaired even in the upper suprabasal layers of bioengineered epidermis when prepared with stiffer scaffold or keratinocytes expressing MKK7-JNK1. By contrast, shJNK1 or shJNK2 epidermis exhibited strong AJ even in the basal layer. The results with bioengineered epidermis were in full agreement with the epidermis of *jnk1*$^{-/-}$ or *jnk2*$^{-/-}$ mice. In conclusion, we propose that JNK mediates the effects of substrate stiffness on AJ formation in 2D and 3D contexts *in vitro* as well as *in vivo*.

Key words: Human primary keratinocytes, Adherens junctions, Intercellular interactions, Substrate rigidity, Bioengineered epidermis, E-cadherin, β-catenin, p-c-Jun

Introduction

c-Jun N-terminal kinases (JNKs), also known as the stress-activated protein kinase, belongs to the mitogen-activated protein kinase (MAPK) superfamily, which also include the ERKs and the p38 MAPKs. The JNKs family includes three members JNK1, JNK2 and JNK3. The *Jnk1* and *Jnk2* genes are expressed ubiquitously in all tissues, whereas *Jnk3* is only expressed in brain, heart and testis (Davis, 2000). It has been well-established that JNKs are activated by MAP2 kinases such as MKK-4, MKK-6 and MKK-7 (Fanger et al., 1997) and regulate cell apoptosis (Hu et al., 1999; Yu et al., 2004), stress response (Leppä and Bohmann, 1999) and cell migration (Nasrazadani and Van Den Berg, 2011). In particular, JNK phosphorylation has been associated with formation of focal adhesions (FA), cell migration, cancer progression and metastasis (Huang et al., 2003; Kimura et al., 2008; Mitra et al., 2011; Nasrazadani and Van Den Berg, 2011). On the other hand, knocking down JNK1 (Zhang et al., 2011) or JNK2 (Mitra et al., 2011) greatly reduced tumor cell migration and invasion, possibly by reducing phosphorylation of the FA adaptor protein, paxillin, ultimately reducing cell motility (Huang et al., 2003).

Our previous work showed JNK phosphorylated β-catenin and regulated adherens junction (AJ) formation in human primary keratinocytes (hKC), epidermoid carcinoma cells (A431) and epidermoid cervical carcinoma cells (ME180) and intestinal epithelial cells (Lee et al., 2009; Lee et al., 2011; Naydenov et al., 2009). Inhibition of JNK activity caused translocation of E-cadherin/β-catenin complex to cell–cell contact sites, leading to formation of AJ, dissociation of α-catenin from E-cadherin/β-catenin complex and actin bundle formation underneath the cell membrane (Lee et al., 2009; Lee et al., 2011). Besides JNK, inhibition of its upstream effector Src family kinase (SFK) also promoted formation of dense AJ in MCF-7 cells (Tsai and Kam, 2009). In addition to mammalian cells, activation of JNK was reported to result in downregulation of E-cadherin and β-catenin complex, loss of cell polarity and tumor growth in Drosophila epithelial cells (Igaki et al., 2006). These data suggest that JNK activity is involved in AJ formation in various epithelial cell types.

Previous studies have shown that there is cross-talk between cell–cell and cell–substrate adhesion as manifested by inhibition of cadherin function upon integrin engagement (Chen and Gumbiner, 2006; Tsai and Kam, 2009). This delicate balance between integrin and cadherin signaling was found to be regulated by substrate rigidity (Tsai and Kam, 2009), which is known to regulate cell spreading, migration, proliferation, stem cell differentiation, and tissue maintenance (Buxboim and Discher, 2010; Guo et al., 2006). Extracellular matrix stiffening has been shown to increase integrin expression and drive malignant behavior of tumor cells through Rho-mediated cytoskeletal tension (Ng and Brugge, 2009; Paszek et al., 2005). Tumor invasiveness was also associated with reduced E-cadherin expression and dissolution of AJ (Sawada et al., 2008;

Siitonen et al., 1996). Recently, we reported that AJ formation/dissolution is regulated by JNK in a swift and dynamic manner, revealing a previously unknown link between JNK and AJ (Lee et al., 2009; Lee et al., 2011).

In the present study, we provide evidence that JNK mediates the effect of surface rigidity on formation/dissolution of AJ in 2D cell culture, in 3D bioengineered tissues *in vitro* as well as in mouse and human epidermis *in vivo*. Our results may have possible implications in understanding epithelial development, wound healing and cancer progression.

Results

Substrate rigidity influences colony formation of epidermal keratinocytes and ME180 cells

Previous studies have shown that substrate rigidity regulated cell–cell adhesion and cell–substrate adhesion, which plays an important role in cell differentiation, cancer metastasis, and formation and maintenance of tissues (Guo et al., 2006; Paszek et al., 2005; Tsai and Kam, 2009; Young et al., 2003). Recent studies from our group showed that JNK regulated formation of AJ in human epidermal keratinocytes (hKC) and other epithelial cell lines in a swift manner (Lee et al., 2009; Lee et al., 2011). In agreement with our previous results, treatment of hKC with the JNK chemical inhibitor, SP600125 induced translocation of E-cadherin and β-catenin to the cell–cell contact sites (Fig. 1A) and actin reorganization into actin cables right beneath the newly formed AJ (Lee et al., 2009). On the other hand, the human epidermoid cervical carcinoma cells (ME180) lacking α-catenin, did not respond to SP600125. However, introduction of α-catenin (ME180 α-catenin) restored the responsiveness of these cells to SP600125 (supplementary material Fig. S1A) suggesting that α-catenin was necessary for AJ formation in response to JNK inhibition.

Here we hypothesized that JNK may regulate cell–cell adhesion in a manner that depends on substrate mechanics. To address this hypothesis, we generated polydimethylsiloxane (PDMS) substrates of different compliance by varying the ratio of polymer to crosslinker. Specifically, we employed substrates with Young's modulus ranging from 1×10^3 kPa to 16 kPa using curing ratios ranging from 9:1 to 49:1 (v/v), respectively (Fig. 1B). As control, we used plastic with Young's modulus of 2.8×10^6 kPa or glass with Young's modulus of 6.9×10^7 kPa (Callister, 2001). Before seeding hKC, substrates were pre-coated with type I collagen (50 μg/ml) for 12 hours at 4℃ followed by UV-treatment for 4 hours. Measurements of fluorescence intensity of surface bound FITC-conjugated collagen showed that similar amounts of collagen were deposited on all surfaces (Fig. 1C). In agreement, the level of phosphorylated focal adhesion kinase (p-FAK) at 30 minutes post-seeding was similar among the substrates, indicating similar levels of initial cell attachment (supplementary material Fig. S2). Indeed, the MTT assay showed that similar numbers of cells adhered on each substrate ($n=3$, $P>0.05$) (Fig. 1D).

On the other hand, substrate stiffness affected hKC morphology significantly (Fig. 1E). On plastic, hKC spread and distributed evenly within 24 hours. However, on the hard PDMS substrate (1×10^3 kPa) hKC tended to form colonies, and further aggregated on soft PDMS (16 kPa). As substrate rigidity decreased the number of single cells decreased and the number of cells participating in colonies increased (Fig. 1F). Interestingly, ME180 lacking α-catenin failed to form colonies but introduction of α-catenin restored the ability of these cells to cluster into colonies on hard and soft PDMS substrates (supplementary material Fig. S1B), suggesting that α-catenin was necessary for AJ formation in response to substrate stiffness, in agreement with our previous findings (Lee et al., 2011).

AJ formation is regulated by substrate mechanics

To confirm that soft substrates induced AJ formation, we employed immunostaining for E-cadherin and β-catenin (Fig. 1G). Plating hKC on PDMS (1×10^3 kPa) induced localization of E-cadherin and β-catenin at the cell–cell contact sites indicating AJ formation. Cell aggregation appeared more compact and the fluorescence staining intensity increased further on the softer PDMS substrate (16 kPa), indicating an inverse relationship between substrate rigidity and AJ formation. The spreading area of cells on soft PDMS was reduced significantly compared to cells on glass (Fig. 1H). As expected, hKC failed to form AJ on glass surface, except when JNK activity was inhibited by treatment of SP600125 (10 μM, 30 minutes).

In contrast to hKC, ME180 cells lacking α-catenin failed to form AJ either with SP600125 treatment or on PDMS substrates, as indicated by E-cadherin immunostaining (supplementary material Fig. S1C). However, introduction of full-length α-catenin restored the ability of ME180 cells to form AJ upon SP600125 treatment and on PDMS substrate. Finally, overexpression of α-catenin-DsRed fusion protein in ME180 cells enabled real-time monitoring of α-catenin translocation to the newly formed cell–cell contact sites on soft PDMS substrates (supplementary material Movies 1, 2).

Substrate rigidity affects JNK phosphorylation

Next we examined the effect of substrate mechanics on JNK phosphorylation. Initially, adhesion of hKC to the collagen-coated surface induced JNK phosphorylation independent of substrate rigidity (Fig. 2A). At 2 hours, phosphorylated JNK (p-JNK) levels decreased on all substrates to about 30–40% (p-JNK1) or 40–50% (p-JNK2) of the initial level on plastic. At 6 hours, the level of p-JNK remained constant on plastic but continued to decrease on the PDMS substrates and by 24 hours, the level of p-JNK was very low, especially on the soft PDMS substrate (p-JNK1 as % of the level on plastic at time zero: hard PDMS, 20±6%; soft PDMS, 7±4%; p-JNK2: hard PDMS, 29±7%; soft PDMS, 4±4%, $P<0.05$ versus plastic 0 hours) (Fig. 2B,C). Consistently, decreasing substrate rigidity decreased the level of p-JNK at 24 hours post-seeding in a dose-dependent manner (Fig. 2D,E). In agreement with p-JNK, the level of p-FAK remained constant on plastic surface, but decreased on hard and soft PDMS within 24 hours (supplementary material Fig. S2).

However, the total protein levels of E-cadherin and β-catenin remained unaffected by substrate stiffness (Fig. 2F). Similar results were observed in ME180 cells. Specifically, the phosphorylation level of p-JNK1 and p-JNK2 decreased with decreasing substrate stiffness (supplementary material Fig. S1D) but the level of E-cadherin and β-catenin remained unchanged (supplementary material Fig. S1E).

Substrate rigidity regulates AJ formation through JNK

Next we employed both constitutively active and knockdown strategies to determine whether substrate stiffness affected AJ formation through JNK. To this end, hKC were transduced with lentivirus encoding for the fusion protein between JNK1 and its upstream activator, MKK7 (MMK7-JNK1), which

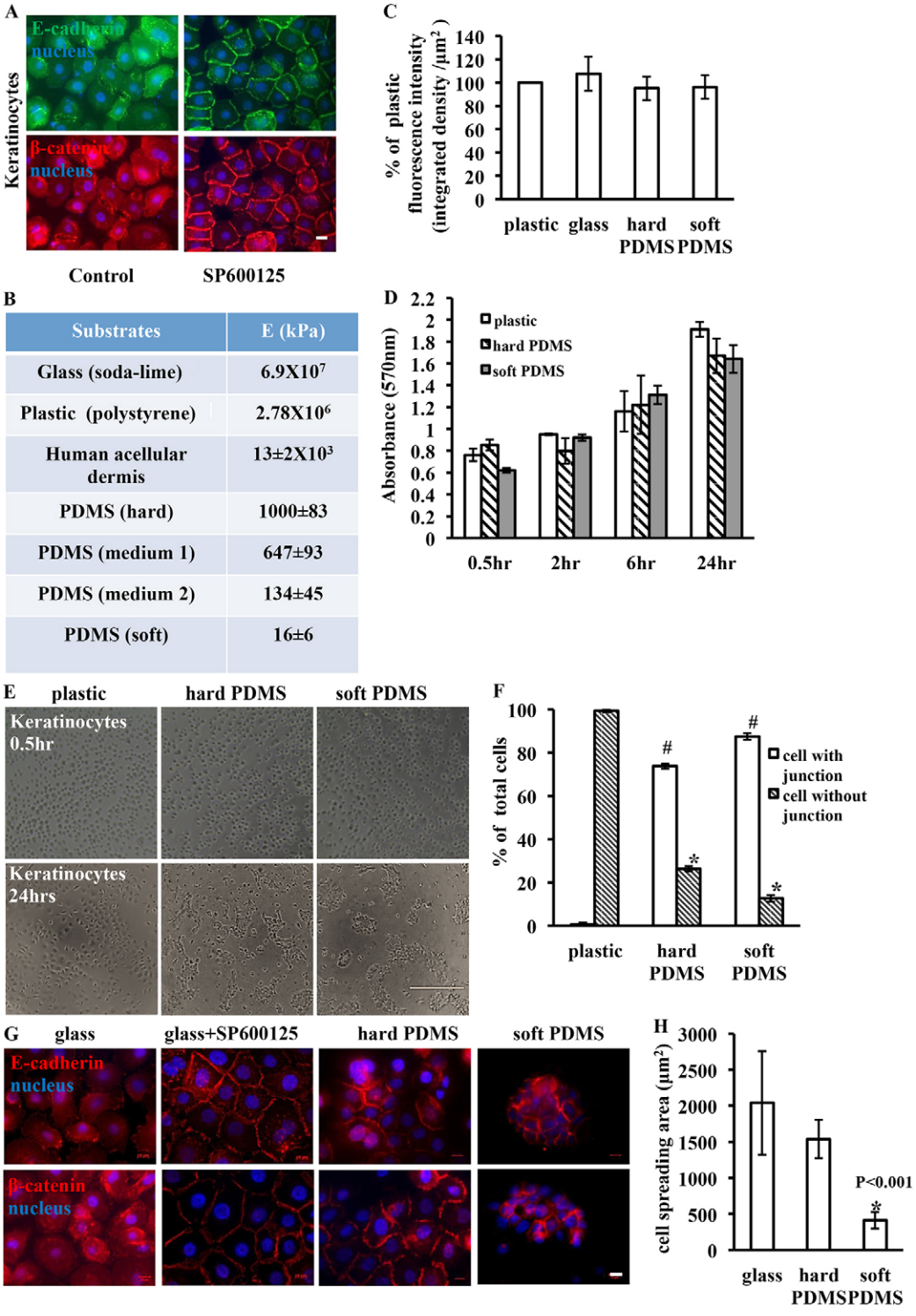

Fig. 1. Substrate rigidity influences colony and AJ formation of epidermal keratinocytes. (**A**) hKC were cultured on a glass surface in the presence or absence of SP600125 (10 μM, 30 minutes) and subsequently immunostained for E-cadherin (green) and β-catenin (red). Nucleus was counterstained with Hoechst dye (blue). View ×63. (**B**) The Young's modulus of human acellular dermis and PDMS substrates of different stiffness were measured by tensile testing (n=3). The Young's modulus of glass and polystyrene were obtained from Callister (Callister, 2001). (**C**) The fluorescence intensity of bound FITC-conjugated collagen on non-tissue culture plastic, glass, hard PDMS and soft PDMS. The data was normalized to the intensity on plastic surface (100%) (n=3). (**D**) Viability of hKC on different substrates was measured by MTT assay at 0.5, 2, 6 and 24 hours post-seeding. Data are presented as absorbance at 570 nm (n=3). (**E**) Morphology of hKC on plastic, hard PDMS or soft PDMS as indicated. View 10×. (**F**) At 24 hours post-seeding, the cells were counted and the percentage of single cells and cells within colonies was determined (n=3); *P<0.001 versus cell without junction on plastic; $^{\#}P$<0.01 versus cell with junction on plastic. (**G**) hKC were cultured on glass surface, hard PDMS and soft PDMS for 24 hours in the presence or absence of SP600125 (10 μM, 30 minutes) and subsequently immunostained for E-cadherin (red) and β-catenin (red). Nuclei were counterstained with Hoechst dye (blue). View 63×. (**H**) At 24 hours post-seeding, the spreading area of hKC on substrates of varying stiffness, i.e. glass, hard PDMS and soft PDMS, was measured using ImageJ (n=3); *P<0.001 versus glass. Scale bars: 10 μm (A,G); 400 μm (E).

was previously shown to increase JNK1 phosphorylation constitutively (Lei et al., 2002). Indeed, expression of MKK7-JNK1 increased the level of p-JNK1 (Fig. 3A) and prevented AJ formation even on the PDMS substrates (Fig. 3B), without affecting the amount of E-cadherin or β-catenin (Fig. 3A). On the other hand, treatment with SP600125 (10 μM) induced AJ formation (Fig. 3B), suggesting that loss of AJ in MKK7-JNK1 cells was due to increased JNK activity.

In addition, we employed shRNA to knockdown JNK1, JNK2 or both JNK1/2 in hKC (Fig. 3C). In agreement with SP600125 treatment, shJNK1, shJNK2 or shJNK1/2 hKC formed AJ not only on hard and soft PDMS but even on glass (Fig. 3D). On the other hand, the amount of total β-catenin and E-cadherin remained unchanged (Fig. 3C). These results demonstrate that the effect of substrate stiffness on cell–cell adhesion and AJ formation may be mediated through JNK.

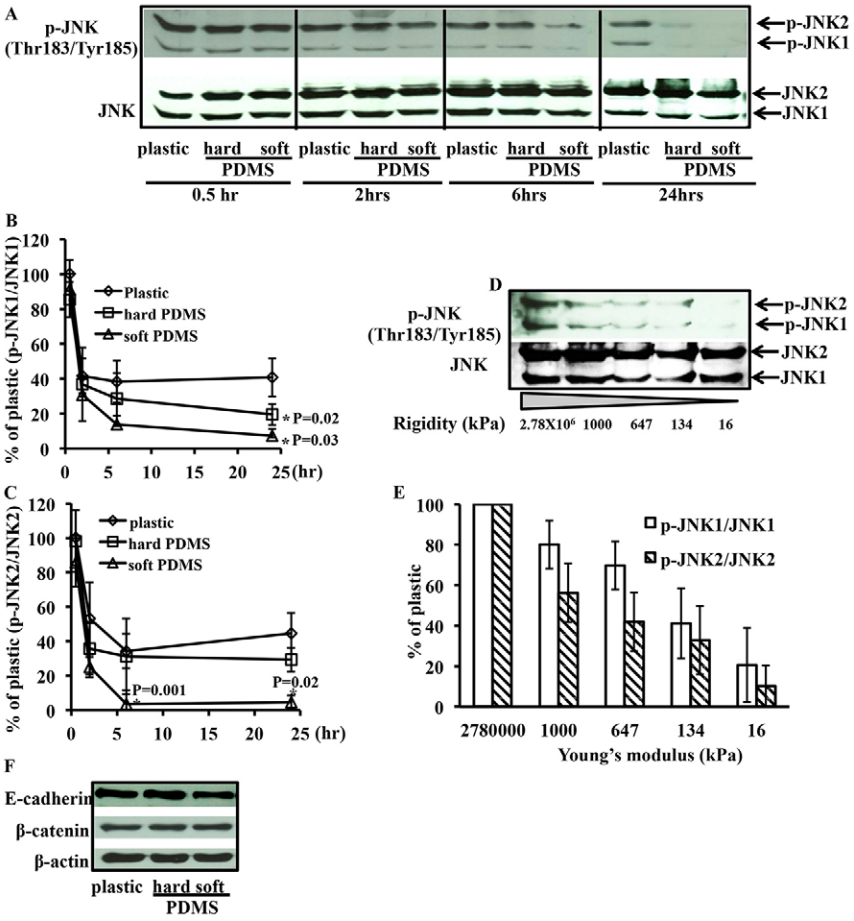

Fig. 2. Substrate rigidity regulates JNK phosphorylation. (**A**) hKC were plated on plastic surface, hard PDMS or soft PDMS. Cell lysates were collected at different time points as indicated and subjected to western blot for p-JNK and JNK. (**B**,**C**) Normalized levels of p-JNK1 (B) or p-JNK2 (C) on varying stiffness substrates. The data were further normalized to the plastic surface at time zero (100%) and plotted as a function of time (n=4); *P<0.05 versus plastic surface (at the same time point). (**D**) hKC were plated on substrates of varying compliance. Cell lysates were collected after 24 hours and subjected to western blot for p-JNK and JNK. (**E**) Lane intensity of p-JNK1 or p-JNK2 at 24 hours post-seeding was quantified and normalized to the expression level of total JNK1 or JNK2, respectively. The data was further normalized to the corresponding level on plastic (100%; n=4). (**F**) hKC were plated on plastic, hard PDMS or soft PDMS substrates. After 24 hours, cell lysates were subjected to western blot for E-cadherin and β-catenin. β-actin served as loading control (n=4).

JNK phosphorylation correlated negatively with AJ formation in human epidermis

Next we examined the relationship between JNK phosphorylation and AJ localization in human neonatal foreskin epidermis. As expected, actively proliferating keratinocytes localized predominately at the basal layer as indicated by proliferating cell nuclear antigen (PCNA) staining, while suprabasal cells stained positive for the differentiation marker, keratin 10 (Fig. 4A). In addition, p-JNK and p-c-Jun were prominently localized in the basal layer but both were also observed in 2–3 suprabasal layers as well (Fig. 4A). On the other hand, immunostaining for E-cadherin, β-catenin, α-catenin and F-actin appeared weak and mostly cytoplasmic in the basal and immediate suprabasal layers but became intense and highly localized at cell–cell contact sites in the upper suprabasal layers (Fig. 4B). Quantification of the fluorescence intensity (arbitrary units/μm^2) of β-catenin at cell–cell contact sites in each epidermal cell layer showed a clear, negative correlation with the levels of p-JNK in nucleus (Spearman correlation coefficient, $R_s = -0.89$), suggesting that JNK may regulate AJ formation in a 3D tissue context as well (Fig. 4C).

Substrate mechanics affect JNK activity and AJ formation in 3D bioengineered tissues

Previous studies indicated that the stratum corneum and dermis are the major contributors to the mechanical integrity of the skin, while the live epidermal cell layers are thought to play only minor role (Magnenat-Thalmann et al., 2002; Pailler-Mattei et al., 2008). Since basal epidermal cells reside on the stiff dermal substrate, while suprabasal cells reside on top of another cell layer, it is plausible that basal cells may experience higher stiffness compared to suprabasal cells. This stiffness gradient may in turn determine the gradients of p-JNK, E-cadherin and β-catenin that were observed across the epidermis. If true, then increasing the stiffness of the dermal substrate might increase the stiffness sensed by basal as well as suprabasal epidermal cells resulting in increased JNK activity and decreased AJ formation in those layers.

To test this hypothesis, we increased the stiffness of the dermal matrix using a natural crosslinker, genipin, which has been used previously to crosslink substrates without toxic effects on the cells. Fig. 5A shows images of crosslinked (dark blue) and control acellular dermis. After degassing and rehydration for 24 hours, the Young's modulus of genipin-crosslinked dermis was 42±4 MPa, which is about threefold higher than control dermis (13±2 MPa) as measured by uniaxial tensile testing (Fig. 5B). After one week of culture at the air-liquid interface, the thickness of bioengineered epidermis was similar on treated and untreated dermis as demonstrated by H&E staining (Fig. 5C,D).

Interestingly, expression of PCNA, p-JNK, and p-c-Jun extended to the upper suprabasal layers of the epidermis grown on genipin-crosslinked dermis. Accordingly, the level of E-cadherin and β-catenin at the cell–cell contact sites was significantly reduced, even in the upper suprabasal layers (Fig. 5E). Quantification of the fluorescence intensity showed that the amount of β-catenin at cell–cell contact sites was significant lower in the suprabasal layers of bioengineered

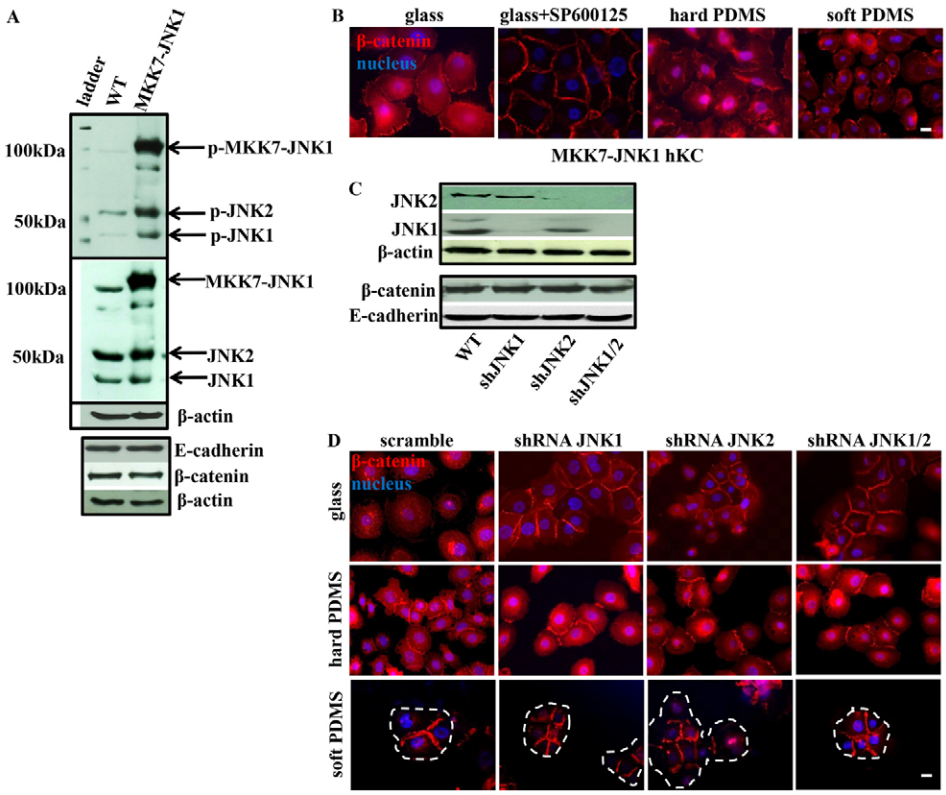

Fig. 3. Substrate rigidity regulates AJ formation through JNK. (**A**) hKC were transduced with a lentiviral vector carrying MKK7-JNK1. Cell lysates were subjected to western blot for p-JNK, JNK, E-cadherin and β-catenin. β-actin served as loading control. (**B**) MKK7-JNK1-transduced hKC were cultured on glass, hard PDMS and soft PDMS in the presence or absence of SP600125 (10 μM, 30 minutes). Cells were immunostained for β-catenin (red) and nucleus was counterstained with Hoechst dye (blue). View 63×. (**C**) hKC were transduced with a lentiviral vector carrying shRNA targeting the *jnk1, jnk2 or jnk1/2* mRNAs. The cell lysates were subjected to western blot for JNK1, JNK2, β-catenin, and E-cadherin proteins. β-actin served as loading control. (**D**) hKC (scramble control, shJNK1, shJNK2 or shJNK1/2) were seeded on glass, hard or soft PDMS. Dash line indicates the colonies. After 24 hours, cells were immunostained for β-catenin (red) and cell nuclei were counterstained with Hoechst dye (blue). View 63×. Scale bars: 10 μm.

epidermis on genipin-treated dermis, as compared to control dermis (Fig. 5F). Notably, decreased AJ formation was accompanied by delayed epidermal differentiation as shown by immunostaining for K10 (Fig. 5E). These results suggest that the increased dermal stiffness was experienced not only by the basal but also suprabasal hKC, leading to increased JNK activity and decreased AJ throughout the epidermis.

Overexpression of JNK disrupted AJ formation in the suprabasal epidermal layers

To verify that the disruption of AJ in the suprabasal cells was due to JNK activation, we generated epidermis with keratinocytes overexpressing the constitutively active, MMK7-JNK1 fusion protein under the control of a doxycycline (Dox)-regulatable promoter. Then MKK7-JNK1 expressing hKC were seeded onto acellular dermis and expression of MKK7-JNK1 was induced by addition of Dox on the first day at the air-liquid interface. On day 7, MKK7-JNK1 cells had formed bioengineered epidermis of similar thickness as control cells (Fig. 6A,B). Immunostaining of tissue sections for E-cadherin and β-catenin showed that MKK7-JNK1 bioengineered epidermis exhibited weak and disorganized AJ (Fig. 6C). The fluorescence intensity of β-catenin at the cell–cell contact sites was significantly lower in the suprabasal layers of MKK7-JNK1 bioengineered epidermis, as compared with control epidermis (Fig. 6D). In agreement, staining for p-JNK, p-c-Jun and the proliferation marker PCNA was extended into the suprabasal layers of MKK7-JNK1 bioengineered epidermis. At the same time, expression of the differentiation marker K10 was restricted only in the upper suprabasal layers, suggesting delayed differentiation (Fig. 6C).

Loss of JNK induced AJ formation in the basal epidermal layer

Next we examined whether eliminating JNK activity was sufficient to induce AJ formation even on the cells of the basal epidermal layer. To test the hypothesis, we employed two 3D model systems: (i) JNK1 and JNK2 knockdown bioengineered epidermis; and (ii) *jnk1*$^{-/-}$ and *jnk2*$^{-/-}$ mice.

First, we prepared bioengineered human epidermis using control (scramble), shJNK1 or shJNK2 hKC. As shown in Fig. 7A,B, shJNK1 bioengineered epidermis contained fewer layers of keratinocytes (shJNK1: 6±1 versus control: 12±2) and was significantly thinner (shJNK1: 77.7±2.2 μm versus control: 95.5±8.5 μm, $P<0.05$), while shJNK2 epidermis showed similar layers but was significantly thicker than control (layer of shJNK2: 13±2, thickness: 124.6±15.5 μm, $P<0.05$). Accordingly, the basal hKC layer in shJNK1 tissue equivalents expressed very low PCNA levels, suggesting low proliferation. In contrast, PCNA staining in shJNK2 epidermis was higher than control and was extended to several suprabasal cell layers (Fig. 7C).

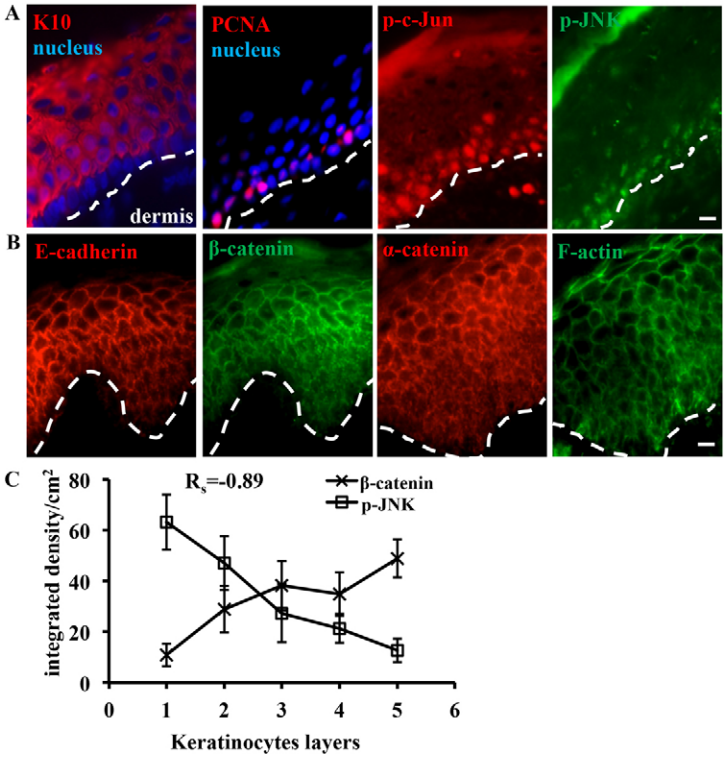

Fig. 4. JNK phosphorylation correlates negatively with AJ formation in human epidermis. (**A**,**B**) Neonatal human foreskin tissues were subjected to immunofluorescence staining for (A) K10 (red), PCNA (red), p-c-Jun (red), p-JNK (green) and (B) E-cadherin (red), β-catenin (green), α-catenin (red) and F-actin (green). Nuclei were counterstained with Hoechst dye (blue). Dashed lines indicate the interface between dermis and epidermis. View 63×. (**C**) Values of fluorescence intensity (integrated density/area) of β-catenin at cell–cell contact sites or p-JNK in nucleus as a function of position in the epidermis. Layer 1 indicates the basal layer. The stratum corneum layers are not included because they do not contain AJ. The Spearman correlation coefficient (R_s=−0.89) denotes a strong negative correlation between p-JNK and β-catenin as a function of position within the epidermis (n=6). Scale bars: 10 μm.

As expected, the levels of p-c-Jun was dramatically reduced in shJNK1 and shJNK2 KC skin equivalents but there was no significant difference in the expression of the differentiation marker K10, which was limited to suprabasal layers similar to native epidermal tissue (Fig. 7C). Interestingly, both shJNK1 and shJNK2 bioengineered epidermis exhibited strong AJ throughout all cell layers including the basal and immediate suprabasal layers, as indicated by E-cadherin and β-catenin staining (Fig. 7C). The fluorescence intensity of β-catenin at cell–cell contact sites was significantly higher in the basal and immediate suprabasal layers of shJNK1 and shJNK2 bioengineered epidermis, as compared with control epidermis (Fig. 7D). Interestingly, increasing the stiffness of acellular dermis by genipin treatment failed to reverse the phenotype of shJNK tissues, which exhibited strong AJ throughout the epidermis including the basal layer (Fig. 7E).

To determine the relevance of our results *in vivo*, we examined the epidermis of *jnk1*$^{-/-}$ and *jnk2*$^{-/-}$ mice. In agreement with the knockdown bioengineered epidermis and with previous reports (Weston et al., 2004), the epidermis of *jnk1*$^{-/-}$ mice contained fewer cell layers compared to control tissues (*jnk1*$^{-/-}$: 3±1 versus WT: 7±2 layers, P<0.05) and was significantly thinner (*jnk1*$^{-/-}$: 5.0±0.9 μm versus WT: 8.8±0.6 μm, P<0.05) (Fig. 7F,G). On the other hand, the *jnk2*$^{-/-}$ mouse epidermis contained similar number of cell layers and it was thicker than wild type but the difference was not significant (*jnk2*$^{-/-}$: 9.5±0.5 μm versus WT: 8.8±0.6 μm) (Fig. 7F,G). As expected, the fluorescence intensity of p-c-Jun was absent in *jnk1*$^{-/-}$ and *jnk2*$^{-/-}$ mouse skin as compared to wild-type mouse epidermis (Fig. 7H). In contrast to native epidermis, both *jnk1*$^{-/-}$ and *jnk2*$^{-/-}$ epidermis exhibited strong AJ in all cell layers including the basal layer (Fig. 7H). In addition, the fluorescence intensity of β-catenin at the cell–cell contact sites of basal cells (layer 1) was significantly higher in *jnk1*$^{-/-}$ and *jnk2*$^{-/-}$ mice, compared to wild-type epidermis (Fig. 7I). Collectively, our results clearly suggest that formation of AJ is regulated by the activity of JNK, which in turn may be regulated by substrate stiffness, ultimately resulting in molecular gradients that may affect tissue stratification and differentiation.

Discussion

Several studies demonstrated that substrate rigidity regulates cell–cell versus cell–substrate adhesion (Discher et al., 2005; Tsai and Kam, 2009). In the present study, we applied glass, plastic and PDMS substrates with varying compliance between 10 and 10^3 kPa to study the effect of stiffness on formation of AJ between epidermal keratinocytes. On rigid glass and plastic surfaces, hKC maintained high levels of JNK activity and spread well but failed to form colonies. On the other hand, on soft PDMS substrates, phosphorylation of JNK decreased over time and cells formed tight colonies within 24 hours. In agreement, immunostaining showed that on rigid surfaces AJ proteins, E-cadherin and β-catenin distributed throughout the cell. In contrast, on soft substrates E-cadherin and β-catenin were localized at the cell–cell contact sites. However, the total amounts of E-cadherin and β-catenin per cell remained unchanged, suggesting that AJ formation on soft substrates did not result from increased synthesis of AJ proteins. These results are in agreement with recent studies implicating substrate stiffness in the disruption of endothelial cell AJ and leading to vascular pathologies such as enhanced permeability, neutrophil transmigration or atherosclerosis (Huynh et al., 2011; Krishnan et al., 2011; Stroka and Aranda-Espinoza, 2011).

Our main finding is that JNK regulates AJ formation in response to substrate stiffness in 2D and 3D culture systems as well as *in vivo*. *In vitro* we observed that the level of JNK

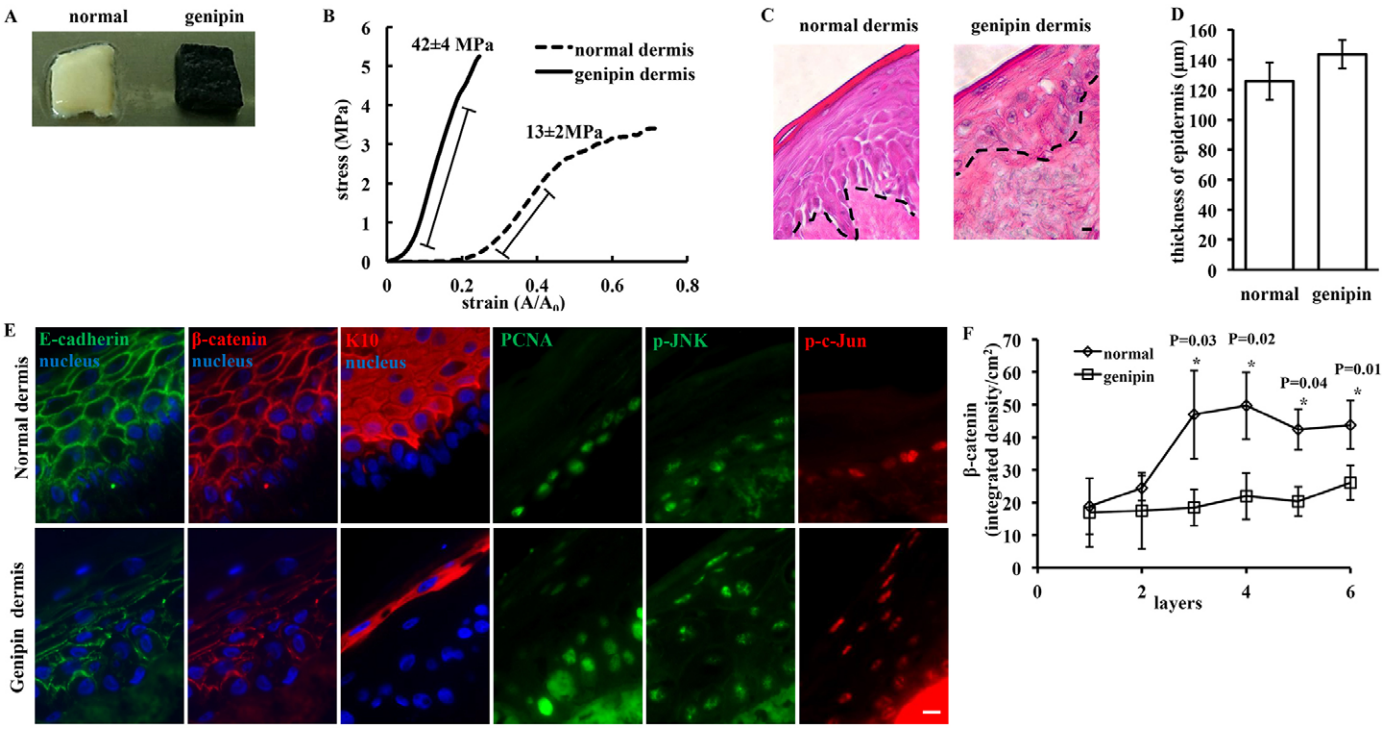

Fig. 5. Substrate mechanics affect JNK activity and AJ formation in 3D tissues. (**A**) Photographs of decellularized dermis before and after genipin treatment (blue). (**B**) Stress-strain relationship of normal and genipin-treated decellularized human dermis as determined by tensile testing. The lines indicate the linear region that was used to calculate the Young's modulus ($n=3$). (**C**) H&E staining of bioengineered skin with normal or genipin-treated dermis. Dashed lines indicate the interface between dermis and epidermis. View 40×. (**D**) The average thickness of the epidermis in C was determined by dividing the area of the tissue by the length of the basement membrane underlying the epidermis ($n=3$). (**E**) The epidermis on normal and genipin-treated dermis were subjected to immunofluorescence staining for E-cadherin (green), β-catenin (red), K10 (red), PCNA (green), p-JNK (green) and p-c-Jun (red). Nuclei were counterstained with Hoechst (blue). View 63×. (**F**) Values of fluorescence intensity of β-catenin at cell–cell contact sites. Layer 1 indicates the basal layer. The stratum corneum layers are not included because they do not contain AJ ($n=3$); *$P<0.05$ versus normal dermis. Scale bars: 10 μm.

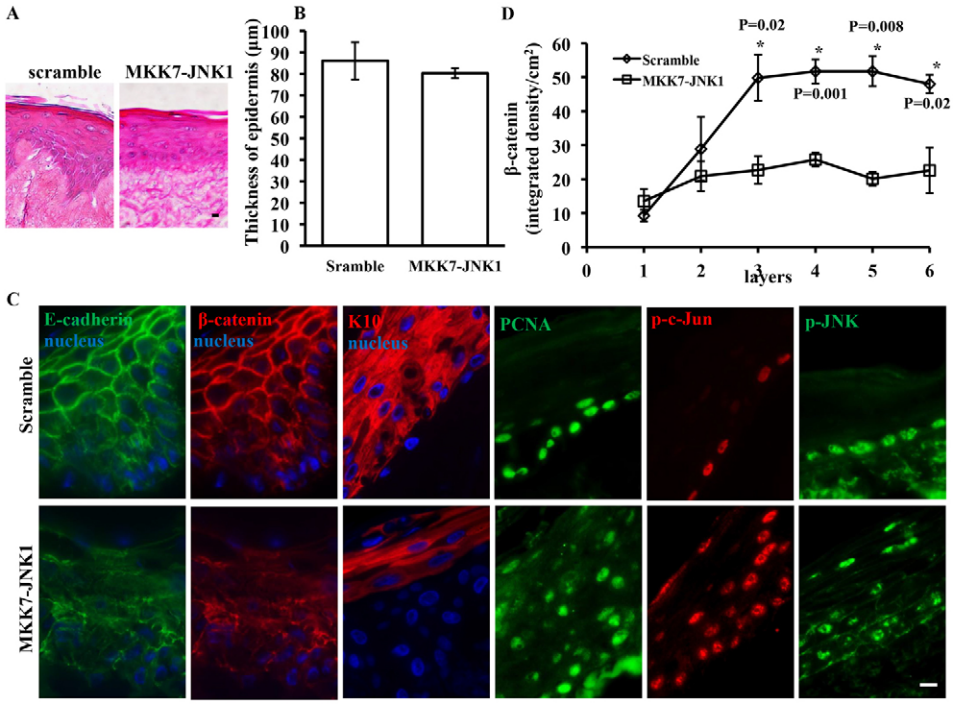

Fig. 6. Overexpression of JNK disrupts AJ formation in the suprabasal epidermal layers. (**A**) H&E staining of scramble and MKK7-JNK1 bioengineered epidermis. View 40×. (**B**) The thickness of epidermis in A ($n=3$). (**C**) Control (scramble) or MKK7-JNK1 skin equivalents were subjected to immunofluorescence staining for E-cadherin (green), β-catenin (red), K10 (red), PCNA (green), p-c-Jun (red) and p-JNK (green). Nuclei were counterstained with Hoechst dye (blue). View 63×. (**D**) Values of fluorescence intensity of β-catenin at cell–cell contact sites. Layer 1 indicates the basal layer. The stratum corneum layers are not included because they do not contain AJ ($n=3$); *$P<0.05$ versus scramble. Scale bars: 10 μm.

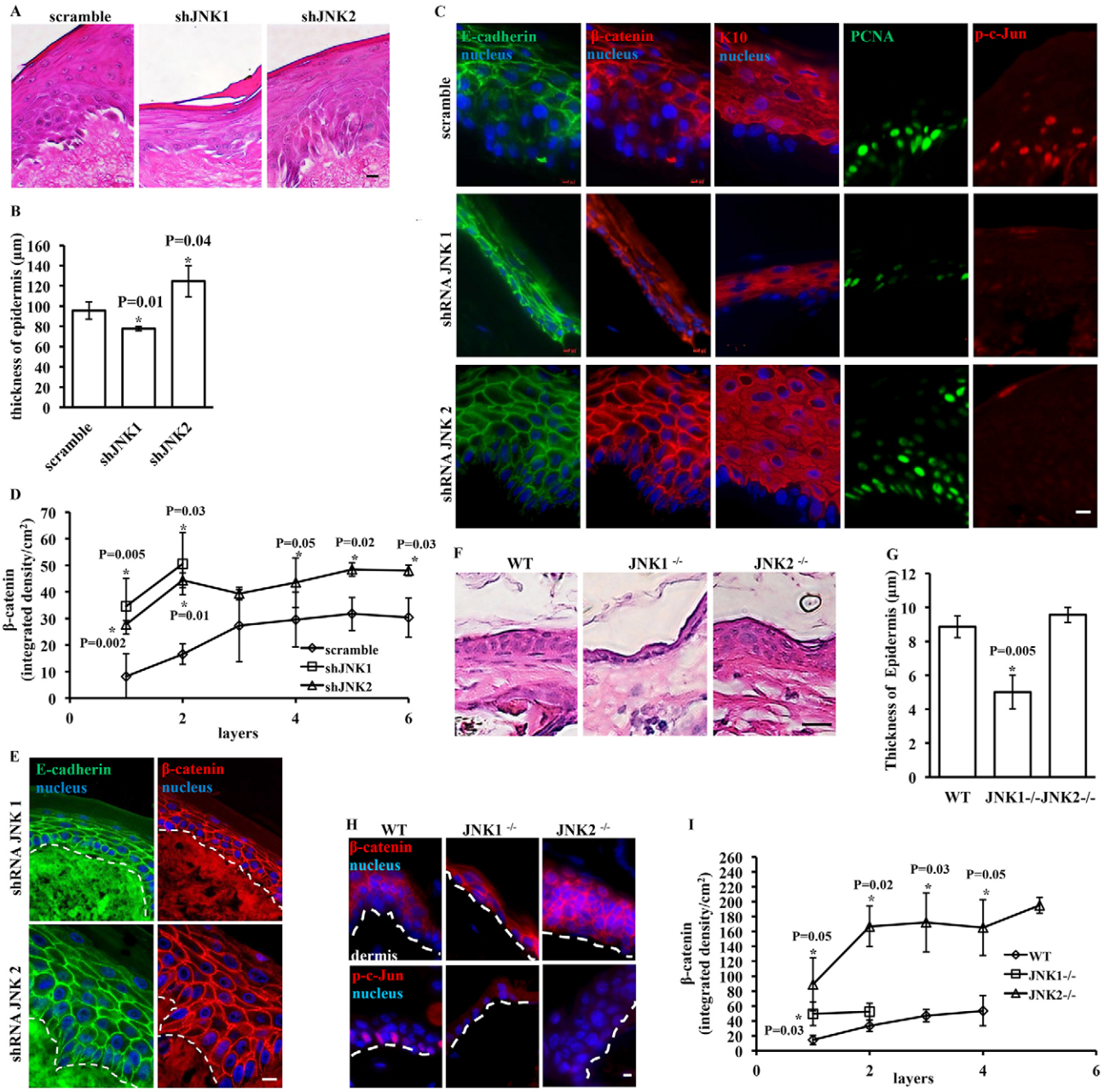

Fig. 7. Loss of JNK induces AJ formation in the basal epidermal layer. (**A**) H&E staining of scramble, shJNK1 and shJNK2 skin equivalents. View 40×. (**B**) The thickness of epidermis in A (n=3). (**C**) Scramble, shJNK1 and shJNK2 epidermal equivalents were immunostained for E-cadherin (green), β-catenin (red), K10 (red), PCNA (green) and p-c-Jun (red). Nuclei were counterstained with Hoechst dye (blue). View 63×. (**D**) Values of fluorescence intensity of β-catenin at cell–cell contact sites. Layer 1 indicates the basal layer. The stratum corneum layers are not included because they do not contain AJ (n=3). (**E**) shJNK1 and shJNK2 epidermal equivalents on genipin-treated dermis were immunostained for E-cadherin (green) and β-catenin (red). Nuclei were counterstained with Hoechst dye (blue). Dashed lines indicate the interface between dermis and epidermis. View 63×. (**F**) H&E staining of wild-type, $jnk1^{-/-}$ or $jnk2^{-/-}$ mouse skin. View 40×. (**G**) Thickness of wild-type, $jnk1^{-/-}$ or $jnk2^{-/-}$ mouse epidermal tissues (n=3). (**H**) Wild-type, $jnk1^{-/-}$ and $jnk2^{-/-}$ mouse skin tissues were immunostained for β-catenin (red), p-c-Jun (red) and nuclei were counterstained with Hoechst dye (blue). View 63×. (**I**) Values of fluorescence intensity of β-catenin at cell–cell contact. Layer 1 indicates the basal layer. The stratum corneum layers are not included because they do not contain AJ (n=3). *P<0.05 versus scramble (B,D) or wild-type (G,I). Scale bars: 10 μm.

phosphorylation decreased with decreasing substrate rigidity. On the softest substrate, JNK phosphorylation was diminished and E-cadherin and β-catenin translocated to the cell–cell contact sites forming AJ. This is in agreement with our previous studies showing that blocking the activity of JNK induced AJ formation in hKC and other epithelial cell lines (Lee et al., 2009; Lee et al., 2011). Indeed, knocking down JNK1, JNK2 or both induced AJ formation even on the hardest substrate, namely the glass surface. Conversely, overexpressing constitutively active JNK prevented AJ formation even on the softest PDMS substrate. Taken together these observations suggest that JNK mediated AJ formation in epithelial cells in response to substrate compliance.

Interestingly, ME180 cells lacking α-catenin did not form AJ on soft substrates. However, introduction of α-catenin restored the ability of ME180 cells (α-cat-ME180) to form substrate-induced AJ. This result is in agreement with recent work from our laboratory demonstrating that α-catenin was necessary for AJ formation in response to JNK inhibition by the chemical inhibitor, SP600125 or by shRNA (Lee et al., 2011). Notably, the level of p-JNK decreased with decreasing substrate stiffness even in ME180 cells that could not form AJ, providing further evidence that JNK inhibition preceded AJ formation. The upstream JNK effector that may be responsive to substrate stiffness in epithelial cells remains to be elucidated, but some studies identified RhoA as substrate-dependent molecular sensor in human bone marrow-derived mesenchymal stem cells and fibroblasts (Huynh et al., 2011; Kim et al., 2009; Krishnan et al., 2011; Paszek et al., 2005; Stroka and Aranda-Espinoza, 2011).

Notably, our *in vitro* data with different substrates in 2D cultures were extended in 3D bioengineered epidermis as well as *in vivo*, suggesting that the epidermis may be experiencing a stiffness gradient. This notion is supported by mechanical testing showing that the major contributor to mechanical integrity of skin tissue comes from the dermis and hypodermis while the contribution of the epidermis is small (Hendriks et al., 2003; Magnenat-Thalmann et al., 2002; Pailler-Mattei et al., 2008). Therefore, the basal cells may be sensing a more rigid substrate (dermis) as compared to the suprabasal and granular cells residing on other, softer epidermal cell layers. This 'cell-on-cell' hypothesis was initially proposed by Discher and colleagues who observed that myotubes attaching on glass showed abundant stress fibers but myotubes cultured on top of another myotube layer differentiated into a striated state, presumably because they perceived a softer substrate (Engler et al., 2004; Griffin et al., 2004). This stiffness gradient across the epidermal tissue may in turn be responsible for downregulating JNK phosphorylation leading to AJ formation in the upper epidermal layers. Indeed, we observed that JNK was phosphorylated in the basal and immediate suprabasal layers but not in the upper suprabasal and granular layers of epidermal tissues (Fig. 4A). In agreement, integrins e.g. α5 and β1 are expressed in the basal epidermal layer but are absent in differentiated keratinocytes of the upper suprabasal layers (Adams and Watt, 1990; Nicholson and Watt, 1991) and significantly downregulated on soft hydrogels (Yeung et al., 2005). Conversely, the reverse gradient was observed for AJ, which were either absent or weak in the basal layer but much stronger in the upper suprabasal layers. Collectively, these data suggest that the molecular gradients of p-JNK and AJ across the epidermis might be the result of a stiffness gradient across the tissue.

To further examine whether substrate stiffness affected JNK phosphorylation and AJ formation throughout the 3D epidermal tissues, we increased the stiffness of the dermis by using the crosslinking agent, genipin. In agreement with previous studies demonstrating genipin biocompatibility (Tsai et al., 2000), we found that the crosslinked substrate could be used to generate bioengineered epidermis of similar thickness as control dermis. Mechanical measurements showed that crosslinking increased the dermal substrate stiffness by threefold. We expected that increased substrate stiffness might increase the stiffness felt not only by the basal cells but also the suprabasal cells residing on top of them (Buxboim et al., 2010; Sen et al., 2009). Indeed, immunostaining showed the presence of p-JNK and p-c-Jun in the upper suprabasal layers of bioengineered epidermis on genipin-treated dermis. At the same time, AJ formation was significantly impaired as indicated by discontinued staining of E-cadherin and β-catenin throughout the tissue. This result suggested that in 3D tissues cells on stiff substrates might be experiencing different rigidity as compared to cells residing on top of other cells, generating a rigidity gradient. This physical gradient may give rise to molecular gradients such as JNK activation and AJ formation, ultimately leading to gradients of cellular function such as proliferation at the basal layer and cell–cell adhesion and differentiation in the suprabasal layers.

Similar to cells in culture, JNK mediated the disruption of AJ in 3D tissues as well. Specifically, expression of constitutively active JNK by hKC led to AJ dissolution throughout the bioengineered epidermis, suggesting that JNK activation was sufficient to disrupt AJ. Conversely, knocking down JNK1 or JNK2 led to AJ formation even at the basal cell layer, which typically does not contain AJ. Interestingly, despite having opposite effects on cell proliferation and epidermal thickness, shJNK1 or shJNK2 had similar effects on AJ formation. Notably, the results in bioengineered epidermis were in agreement with observations in the epidermis of $jnk1^{-/-}$ or $jnk2^{-/-}$ mice. While $jnk1^{-/-}$ epidermis appeared much thinner than $jnk2^{-/-}$ or control epidermis, both $jnk1^{-/-}$ and $jnk2^{-/-}$ tissues showed increased formation of AJ throughout all layers, including the basal cells. Taking together, these data clearly demonstrate that JNK affects AJ formation in 3D tissue constructs as well as *in vivo*, possibly by sensing a stiffness gradient across tissue layers. However, other factors that might also influence JNK activity and AJ formation *in vivo*, e.g. the reduction of pore size in genipin-crosslinked ECM scaffolds such as acellular dermis (Trappmann et al., 2012), nutrient or calcium concentration gradients across the epidermis cannot be presently excluded.

In agreement with a previous study (Weston et al., 2004), $jnk1^{-/-}$ mice displayed significantly thinner epidermis, with markedly reduced proliferation in the basal cell layer. Differentiation markers, such as keratohyalin granules, loricrin and keratin 6 were missing in the $jnk1^{-/-}$ mouse skin. On the other hand, mice lacking JNK2 exhibited epidermal hyperplasia resulting in thicker epidermal layer containing increased fraction of p63+ cells. Some differentiation markers such as keratin 10 and keratohyalin granules remained similar to wild-type mice, while others such as loricrin and keratin 6 were even upregulated (Weston et al., 2004). Another study documented the differential effects of JNK1 *versus* JNK2 on proliferation (Sabapathy et al., 2004). Various cell types including fibroblasts, erythroblasts and hepatocytes from $jnk2^{-/-}$ mice were found to exhibit increased proliferation rates compared to their wild-type counterparts. In contrast, JNK1 is the positive regulator of c-Jun, and as a result loss of JNK1 leads to decreased proliferation.

Notably, JNK, an important regulator of cell migration, is engaged in both focal adhesion and adherens junction processes. JNK is one of the downstream targets of integrin and focal adhesion kinase (FAK) (Oktay et al., 1999) and it is known to phosphorylate serine 178 on paxillin, a focal adhesion adaptor protein (Huang et al., 2003). Interestingly, on soft substrates hKC spread much less indicating reduced integrin engagement. Indeed, FAK phosphorylation also decreased on the hard and most noticeably on the soft PDMS substrate (supplementary material Fig. S2), in agreement with previous results (Evans et al., 2009). On the other hand, our previous findings showed that JNK

phosphorylated β-catenin and inhibition of JNK activity caused translocation of the E-cadherin/β-catenin complex to cell–cell contact sites, leading to formation of AJ (Lee et al., 2009; Lee et al., 2011). Taken together, these data suggest the hypothesis that JNK may be a switch regulating the balance between adherens junctions and focal adhesions. This hypothesis requires further investigation.

Collectively, our results may have implications in epithelial tumor development as accumulating evidence suggests that both tumor cells and their stroma displayed increased stiffness as compared to their normal counterparts (Levental et al., 2009; Paszek et al., 2005; Samuel et al., 2011). Stiff stroma was shown to drive focal adhesions, disrupt AJ, perturb tissue polarity, and promote growth and malignant behavior both *in vitro* and *in vivo* (Ng and Brugge, 2009; Paszek et al., 2005). JNK has also been implicated in several cancers including melanoma, head and neck, breast, gastric and ovarian cancers (Alexaki et al., 2008; Potapova et al., 2000a; Potapova et al., 2000b; Shibata et al., 2008; Yang et al., 2003); while chemical inhibition of JNK inhibited growth of head and neck squamous cell carcinoma (Gross et al., 2007) and ovarian cancer (Vivas-Mejia et al., 2010). Finally, in many epithelial tumors such as gastric, breast, pancreatic and ovarian cancers, E-cadherin expression was partially or completely lost as they moved towards malignancy (Berx and van Roy, 2009). Taken together our data may provide the missing link between substrate stiffness and cancer progression from benign to malignant through substrate-mediated activation of JNK, ultimately leading to loss of AJ and acquisition of metastatic phenotype. More work is required to address this interesting hypothesis.

Materials and Methods

Materials

The antibody for K10 was purchased from Abcam (Cambridge, MA). SP600125 was purchased from Enzo Life Sciences INC. (Plymouth Meeting, PA). E-cadherin, β-catenin, JNK, p-c-Jun, FAK (Tyr397), and FAK antibodies were from Cell Signaling (Danvers, MA). Type I collagen and p-JNK (Thr183/Tyr185) antibodies were from BD Biosciences (San Jose, CA). JNK1 and JNK2 antibodies were from Santa Cruz Biotechnology (Santa Cruz, CA). Genipin, FluoroTag™ FITC Conjugation Kit, 3-(4,5-dimethylthiazol-2-yl)-2,5-diphenyltetrazolium bromide (MTT), and β-actin antibody were purchased from Sigma-Aldrich (St. Louis, MO). The antibody for Proliferating Cell Nuclear Antigen (PCNA) was from BioLegend (San Diego, CA). Hoechst 33342, Alexa Fluor® 488 Phalloidin and Alexa Fluor® 488/594 Goat Anti-Rabbit/Mouse IgG (H^+L) antibodies were from Life Technologies (Grand Island, NY). Polydimethylsiloxane (PDMS) substrates were produced with the SYLGARD® 184 silicone elastomer kit from Dow Corning Corporation (Midland, MI). Wild-type, *jnk1*$^{-/-}$ and *jnk2*$^{-/-}$ mice were generated as described previously (Dong et al., 1998; Yang et al., 1998).

PDMS preparation

PDMS substrates of variable stiffness were fabricated using the SYLGARD® 184 silicone elastomer kit as per the manufacturer's instructions with curing ratios (polymer to crosslinker): 9:1(hard), 11.5:1 (medium 1), 24:1 (medium 2) or 49:1 (soft) (v/v). Mixed and degassed solutions were then poured into 6-well plates to a depth of at least 1 mm and cured at 45℃ for 24 hours. Cured PDMS preparations, non-tissue culture plastic surface and glass surface were coated with type I collagen (0.05 mg/ml) for 12 hours at 4℃ followed by UV treatment for 4 hours. Before seeding cells, collagen-coated surfaces were washed with PBS twice.

MTT assay

hKC (20,000 cells/well) were seeded on plastic surface or PDMS substrates polymerized in 96-well plates. After 0.5, 2, 6, and 24 hours the medium was replaced with 200 µl of fresh medium containing 1 mg/ml of MTT. After 1 hour of incubation at 37℃, the MTT-containing medium was removed, and the reduced formazan dye was solubilized by adding 100 µl of DMSO to each well. After gentle mixing, the absorbance was measured at 570 nm using a multi-well plate reader (SYNERGY 4, BioTek, Winooski, VT).

Cell culture and bioengineered skin equivalents

hKC were isolated from neonatal human foreskins, as described before (Koria and Andreadis, 2006) and cultured in serum free medium (EpiLife® Medium with 60 µM calcium, Life Technologies). ME180 cells were cultured and passaged routinely in DMEM supplemented with 10% FBS.

To obtain decellularized human dermis (DED), human cadaver skin was subjected to three freeze/thaw cycles: 10 minutes in liquid nitrogen followed by 30 minutes at 37℃. After three washes in PBS, the skin was incubated in an antibiotic cocktail containing 0.1 mg/ml of Gentamycin, 10 µg/ml of Ciprofloxacin, 100 units/ml of penicillin, 100 µg/ml of streptomycin, and 0.25 µg/ml of amphotericin B at 37℃. One week later, the epidermis was peeled off, and the DED was incubated in fresh antibiotic cocktail at 4℃ for four weeks before use (Medalie et al., 1997; Andreadis et al., 2001). Bioengineered skin equivalents were prepared as described previously (Andreadis et al., 2001). Briefly, hKC growing on mouse fibroblast feeder layer (3T3/J2, ATCC, Manassas, VA) were seeded onto acellular dermis and raised to the air-liquid interface for 7 days.

Crosslinking acellular dermis

To prepare tissue engineered skin, the DED was cut into 1 cm^2 square pieces and were treated with genipin (0.5% w/v in PBS) at room temperature for 96 hours. Control pieces were soaked in PBS without genipin for the same amount of time. Following treatment with genipin, DED pieces were washed extensively with PBS, degassed to remove genipin that was trapped within the pores of the material and rehydrated in PBS before use.

Lentiviral expression constructs

shRNA targeting the *jnk1*, *jnk2*, and *jnk1/2* mRNAs (target sequence: *jnk1:* 5′-GGGCCTACAGAGAGCTAGTTCTTAT-3′, *jnk2:* 5′-GCCAACTGTGAGGAA-TTATGTCGAA-3′, *jnk1/2:*5′-AAAGAAUGUCCUACCUUCU-3′) was cloned downstream of the H1 promoter between the *Mlu*I and *Cla*I sites of the pLVTHM lentiviral vector (Wiznerowicz and Trono, 2003). This vector also encodes for EGFP under the EF1α promoter, which was used to select for shRNA expressing cells using flow cytometry (Lee et al., 2009). A fusion protein of JNK and its upstream activator MKK7 was cloned in downstream of the CMV promoter between *Age*I and *Mlu*I sites of the p-TRIP-Z vector (Open Biosystems, Huntsville, AL). Cells were selected by puromycin treatment and doxycycline (1 µg/ml) was used to induce MKK7-JNK1 protein expression.

Mechanical characterization of PDMS and DED

PDMS thin strips (~40 mm×5 mm×1 mm) and DED strips (~20 mm×5 mm×2 mm) were subjected to uniaxial testing using Instron 3343 (Instron®, Norwood, MA) equipped with 50N load cell. The data were analyzed using Bluehill® 3 software and the elastic modulus was determined from the slope of the linear part of the stress-strain curves.

Immunoblotting

Cells lysates were prepared essentially as described previously (You and Laychock, 2009). Equal amounts of protein per sample (30–40 µg) for each experiment were separated on 8% SDS-PAGE gels and transferred to PVDF (0.45 µm) membranes. Immunoblotting was carried out essentially as described previously (You and Laychock, 2009). PVDF membranes were incubated with primary antibodies (p-JNK, JNK, JNK1, JNK2, E-cadherin, β-catenin, p-FAK, FAK, and β-actin; dilution 1:1000) for overnight at 4℃, and horseradish peroxidase (HRP)-conjugated anti-rabbit/mouse IgG secondary antibody (dilution 1:1000) for 1 hour at room temperature.

Immunofluorescence and confocal microscopy

hKC and ME180 cells or tissue sections (paraffin-embedded or OCT-embedded cryosections) of human neonatal foreskin, mouse skin or bioengineered skin were fixed with paraformaldehyde (4% w/v) and permeabilized with (0.1% v/v) Triton X-100. After incubation with blocking buffer (5% v/v goat serum in PBS), samples were incubated with the primary antibodies against: E-cadherin, β-catenin, K10, PCNA, p-c-Jun, p-JNK, α-catenin (dilution 1:100 in blocking buffer) or Alexa Fluor® 488 phalloidin (dilution 1:40 in blocking buffer) overnight at 4℃. Cells or tissues were washed at least three times and treated with secondary antibodies: Alexa Fluor® 488 goat anti-rabbit/mouse IgG (H^+L) (1:200 dilution) or Alexa Fluor® 594 goat anti-rabbit/mouse IgG (H^+L) (1:400 dilution) for 1 hour at room temperature. Samples were imaged with Zeiss AxioObserver.Z1 fluorescence microscope equipped with a digital camera (ORCA-ER C4742-80; Hamamatsu, Bridgewater, NJ) or confocal microscope (LSM 510; Zeiss, Oberkochen, Germany) equipped with a digital camera. Finally, images were analyzed using the ImageJ software.

Analysis of fluorescence intensity of human neonatal foreskin, mouse skin and human bioengineered skin tissues sections

Since the thickness of the epidermis and cell orientation may vary from point to point within the tissue, the following procedure was used to quantify fluorescence

intensity at each cell layer. First, a box was set such that it was perpendicular to the stratum corneum layer and its width was about the same as the width of a cell. In each cell within the box, two circles were manually drawn, one corresponding to the nucleus (blue, Hoechst) and the other surrounding the cell membrane (green, β-catenin) and measured the fluorescence intensity and area between the two circles. The fluorescence intensity between two cells (i.e. at the junction) was assigned to both cells. These measurements did not include the stratum corneum, which is composed of cornified, non-living cells.

Statistical analysis

All statistical analysis was performed using the Statmost statistical analysis software (Dataxiom Software Inc., Los Angeles, CA). Values are means ± s.e.m. Significant differences between treatment groups were determined by Student's *t*-test (paired, two-tailed) or one-way analysis of variance (ANOVA) with post-hoc analysis using Student–Newman–Keuls multiple comparison test or Spearman correlations analysis. Values of $P \leq 0.05$ were accepted as significant.

Author contributions

H.Y. performed experiments, and was involved in collection and/or assembly of data, data analysis and interpretation, and manuscript writing. R. P. performed experiments, and was involved in collection and/or assembly of data, data analysis and interpretation. A.R. performed experiments, and was involved in collection and/or assembly of data. P.L. was involved in data interpretation and manuscript writing. N.G. performed experiments. R.J.D. was involved in data interpretation and manuscript writing. S.T.A. was responsible for conception and design, data analysis and interpretation, manuscript writing and final approval of manuscript.

Funding

This work was supported in part by a grant from the National Science Foundation [grant number BES-0354626] to S.T.A. The confocal microscopy imaging facility was supported by a Major Research Instrumentation (MRI) grant from the National Science Foundation [grant number DBI 0923133].

Supplementary material available online at
http://jcs.biologists.org/lookup/suppl/doi:10.1242/jcs.122903/-/DC1

References

Adams, J. C. and Watt, F. M. (1990). Changes in keratinocyte adhesion during terminal differentiation: reduction in fibronectin binding precedes alpha 5 beta 1 integrin loss from the cell surface. *Cell* **63**, 425-435.

Alexaki, V. I., Javelaud, D. and Mauviel, A. (2008). JNK supports survival in melanoma cells by controlling cell cycle arrest and apoptosis. *Pigment Cell Melanoma Res.* **21**, 429-438.

Andreadis, S. T., Hamoen, K. E., Yarmush, M. L. and Morgan, J. R. (2001). Keratinocyte growth factor induces hyperproliferation and delays differentiation in a skin equivalent model system. *FASEB J.* **15**, 898-906. http://doi:10.1096/fj.00-0324com

Berx, G. and van Roy, F. (2009). Involvement of members of the cadherin superfamily in cancer. *Cold Spring Harb. Perspect. Biol.* **1**, a003129.

Buxboim, A. and Discher, D. E. (2010). Stem cells feel the difference. *Nat. Methods* **7**, 695-697.

Buxboim, A., Rajagopal, K., Brown, A. E. and Discher, D. E. (2010). How deeply cells feel: methods for thin gels. *J. Phys. Condens. Matter* **22**, 194116.

Callister, W. D. (2001). Fundamentals of Materials Science and Engineering: an interactive etext. New York: Wiley.

Chen, X. and Gumbiner, B. M. (2006). Crosstalk between different adhesion molecules. *Curr. Opin. Cell Biol.* **18**, 572-578.

Davis, R. J. (2000). Signal transduction by the JNK group of MAP kinases. *Cell* **103**, 239-252.

Discher, D. E., Janmey, P. and Wang, Y. L. (2005). Tissue cells feel and respond to the stiffness of their substrate. *Science* **310**, 1139-1143.

Dong, C., Yang, D. D., Wysk, M., Whitmarsh, A. J., Davis, R. J. and Flavell, R. A. (1998). Defective T cell differentiation in the absence of Jnk1. *Science* **282**, 2092-2095.

Engler, A. J., Griffin, M. A., Sen, S., Bönnemann, C. G., Sweeney, H. L. and Discher, D. E. (2004). Myotubes differentiate optimally on substrates with tissue-like stiffness: pathological implications for soft or stiff microenvironments. *J. Cell Biol.* **166**, 877-887.

Evans, N. D., Minelli, C., Gentleman, E., LaPointe, V., Patankar, S. N., Kallivretaki, M., Chen, X., Roberts, C. J. and Stevens, M. M. (2009). Substrate stiffness affects early differentiation events in embryonic stem cells. *Eur. Cell. Mater.* **18**, 1-13, discussion 13-14.

Fanger, G. R., Gerwins, P., Widmann, C., Jarpe, M. B. and Johnson, G. L. (1997). MEKKs, GCKs, MLKs, PAKs, TAKs, and tpls: upstream regulators of the c-Jun amino-terminal kinases? *Curr. Opin. Genet. Dev.* **7**, 67-74.

Griffin, M. A., Sen, S., Sweeney, H. L. and Discher, D. E. (2004). Adhesion-contractile balance in myocyte differentiation. *J. Cell Sci.* **117**, 5855-5863.

Gross, N. D., Boyle, J. O., Du, B., Kekatpure, V. D., Lantowski, A., Thaler, H. T., Weksler, B. B., Subbaramaiah, K. and Dannenberg, A. J. (2007). Inhibition of Jun NH2-terminal kinases suppresses the growth of experimental head and neck squamous cell carcinoma. *Clin. Cancer Res.* **13**, 5910-5917.

Guo, W. H., Frey, M. T., Burnham, N. A. and Wang, Y. L. (2006). Substrate rigidity regulates the formation and maintenance of tissues. *Biophys. J.* **90**, 2213-2220.

Hendriks, F. M., Brokken, D., van Eemeren, J. T., Oomens, C. W., Baaijens, F. P. and Horsten, J. B. (2003). A numerical-experimental method to characterize the non-linear mechanical behaviour of human skin. *Skin Res. Technol.* **9**, 274-283.

Hu, Y. L., Li, S., Shyy, J. Y. and Chien, S. (1999). Sustained JNK activation induces endothelial apoptosis: studies with colchicine and shear stress. *Am. J. Physiol.* **277**, H1593-H1599.

Huang, C., Rajfur, Z., Borchers, C., Schaller, M. D. and Jacobson, K. (2003). JNK phosphorylates paxillin and regulates cell migration. *Nature* **424**, 219-223.

Huynh, J., Nishimura, N., Rana, K., Peloquin, J. M., Califano, J. P., Montague, C. R., King, M. R., Schaffer, C. B. and Reinhart-King, C. A. (2011). Age-related intimal stiffening enhances endothelial permeability and leukocyte transmigration. *Sci. Transl. Med.* **3**, 112ra122.

Igaki, T., Pagliarini, R. A. and Xu, T. (2006). Loss of cell polarity drives tumor growth and invasion through JNK activation in Drosophila. *Curr. Biol.* **16**, 1139-1146.

Kim, T. J., Seong, J., Ouyang, M., Sun, J., Lu, S., Hong, J. P., Wang, N. and Wang, Y. (2009). Substrate rigidity regulates Ca2+ oscillation via RhoA pathway in stem cells. *J. Cell. Physiol.* **218**, 285-293.

Kimura, K., Teranishi, S., Yamauchi, J. and Nishida, T. (2008). Role of JNK-dependent serine phosphorylation of paxillin in migration of corneal epithelial cells during wound closure. *Invest. Ophthalmol. Vis. Sci.* **49**, 125-132.

Koria, P. and Andreadis, S. T. (2006). Epidermal morphogenesis: the transcriptional program of human keratinocytes during stratification. *J. Invest. Dermatol.* **126**, 1834-1841.

Krishnan, R., Klumpers, D. D., Park, C. Y., Rajendran, K., Trepat, X., van Bezu, J., van Hinsbergh, V. W., Carman, C. V., Brain, J. D., Fredberg, J. J. et al. (2011). Substrate stiffening promotes endothelial monolayer disruption through enhanced physical forces. *Am. J. Physiol. Cell Physiol.* **300**, C146-C154.

Lee, M. H., Koria, P., Qu, J. and Andreadis, S. T. (2009). JNK phosphorylates beta-catenin and regulates adherens junctions. *FASEB J.* **23**, 3874-3883.

Lee, M. H., Padmashali, R., Koria, P. and Andreadis, S. T. (2011). JNK regulates binding of alpha-catenin to adherens junctions and cell–cell adhesion. *FASEB J.* **25**, 613-623.

Lei, K., Nimnual, A., Zong, W. X., Kennedy, N. J., Flavell, R. A., Thompson, C. B., Bar-Sagi, D. and Davis, R. J. (2002). The Bax subfamily of Bcl2-related proteins is essential for apoptotic signal transduction by c-Jun NH(2)-terminal kinase. *Mol. Cell. Biol.* **22**, 4929-4942.

Leppä, S. and Bohmann, D. (1999). Diverse functions of JNK signaling and c-Jun in stress response and apoptosis. *Oncogene* **18**, 6158-6162.

Levental, K. R., Yu, H., Kass, L., Lakins, J. N., Egeblad, M., Erler, J. T., Fong, S. F., Csiszar, K., Giaccia, A., Weninger, W. et al. (2009). Matrix crosslinking forces tumor progression by enhancing integrin signaling. *Cell* **139**, 891-906.

Magnenat-Thalmann, N., Kalra, P., Lévêque, J. L., Bazin, R., Batisse, D. and Querleux, B. (2002). A computational skin model: fold and wrinkle formation. *IEEE Trans. Inf. Technol. Biomed.* **6**, 317-323.

Medalie, D. A., Eming, S. A., Collins, M. E., Tompkins, R. G., Yarmush, M. L. and Morgan, J. R. (1997). Differences in dermal analogs influence subsequent pigmentation, epidermal differentiation, basement membrane, and rete ridge formation of transplanted composite skin grafts. *Transplantation* **64**, 454-465.

Mitra, S., Lee, J. S., Cantrell, M. and Van den Berg, C. L. (2011). c-Jun N-terminal kinase 2 (JNK2) enhances cell migration through epidermal growth factor substrate 8 (EPS8). *J. Biol. Chem.* **286**, 15287-15297.

Nasrazadani, A. and Van Den Berg, C. L. (2011). c-Jun N-terminal Kinase 2 Regulates Multiple Receptor Tyrosine Kinase Pathways in Mouse Mammary Tumor Growth and Metastasis. *Genes Cancer.* **2**, 31-45.

Naydenov, N. G., Hopkins, A. M. and Ivanov, A. I. (2009). c-Jun N-terminal kinase mediates disassembly of apical junctions in model intestinal epithelia. *Cell Cycle* **8**, 2110-2121.

Ng, M. R. and Brugge, J. S. (2009). A stiff blow from the stroma: collagen crosslinking drives tumor progression. *Cancer Cell* **16**, 455-457.

Nicholson, L. J. and Watt, F. M. (1991). Decreased expression of fibronectin and the alpha 5 beta 1 integrin during terminal differentiation of human keratinocytes. *J. Cell Sci.* **98**, 225-232.

Oktay, M., Wary, K. K., Dans, M., Birge, R. B. and Giancotti, F. G. (1999). Integrin-mediated activation of focal adhesion kinase is required for signaling to Jun NH2-terminal kinase and progression through the G1 phase of the cell cycle. *J. Cell Biol.* **145**, 1461-1470.

Pailler-Mattei, C., Bec, S. and Zahouani, H. (2008). In vivo measurements of the elastic mechanical properties of human skin by indentation tests. *Med. Eng. Phys.* **30**, 599-606.

Paszek, M. J., Zahir, N., Johnson, K. R., Lakins, J. N., Rozenberg, G. I., Gefen, A., Reinhart-King, C. A., Margulies, S. S., Dembo, M., Boettiger, D. et al. (2005). Tensional homeostasis and the malignant phenotype. *Cancer Cell* **8**, 241-254.

Potapova, O., Gorospe, M., Bost, F., Dean, N. M., Gaarde, W. A., Mercola, D. and Holbrook, N. J. (2000a). c-Jun N-terminal kinase is essential for growth of human T98G glioblastoma cells. *J. Biol. Chem.* **275**, 24767-24775.

Potapova, O., Gorospe, M., Dougherty, R. H., Dean, N. M., Gaarde, W. A. and Holbrook, N. J. (2000b). Inhibition of c-Jun N-terminal kinase 2 expression suppresses growth and induces apoptosis of human tumor cells in a p53-dependent manner. *Mol. Cell. Biol.* **20**, 1713-1722.

Sabapathy, K., Hochedlinger, K., Nam, S. Y., Bauer, A., Karin, M. and Wagner, E. F. (2004). Distinct roles for JNK1 and JNK2 in regulating JNK activity and c-Jun-dependent cell proliferation. *Mol. Cell* **15**, 713-725.

Samuel, M. S., Lopez, J. I., McGhee, E. J., Croft, D. R., Strachan, D., Timpson, P., Munro, J., Schröder, E., Zhou, J., Brunton, V. G. et al. (2011). Actomyosin-mediated cellular tension drives increased tissue stiffness and β-catenin activation to induce epidermal hyperplasia and tumor growth. *Cancer Cell* **19**, 776-791.

Sawada, K., Mitra, A. K., Radjabi, A. R., Bhaskar, V., Kistner, E. O., Tretiakova, M., Jagadeeswaran, S., Montag, A., Becker, A., Kenny, H. A. et al. (2008). Loss of E-cadherin promotes ovarian cancer metastasis via alpha 5-integrin, which is a therapeutic target. *Cancer Res.* **68**, 2329-2339.

Sen, S., Engler, A. J. and Discher, D. E. (2009). Matrix strains induced by cells: Computing how far cells can feel. *Cell Mol. Bioeng* **2**, 39-48.

Shibata, W., Maeda, S., Hikiba, Y., Yanai, A., Sakamoto, K., Nakagawa, H., Ogura, K., Karin, M. and Omata, M. (2008). c-Jun NH2-terminal kinase 1 is a critical regulator for the development of gastric cancer in mice. *Cancer Res.* **68**, 5031-5039.

Siitonen, S. M., Kononen, J. T., Helin, H. J., Rantala, I. S., Holli, K. A. and Isola, J. J. (1996). Reduced E-cadherin expression is associated with invasiveness and unfavorable prognosis in breast cancer. *Am. J. Clin. Pathol.* **105**, 394-402.

Stroka, K. M. and Aranda-Espinoza, H. (2011). Endothelial cell substrate stiffness influences neutrophil transmigration via myosin light chain kinase-dependent cell contraction. *Blood* **118**, 1632-1640.

Trappmann, B., Gautrot, J. E., Connelly, J. T., Strange, D. G., Li, Y., Oyen, M. L., Cohen Stuart, M. A., Boehm, H., Li, B., Vogel, V. et al. (2012). Extracellular-matrix tethering regulates stem-cell fate. *Nat. Mater.* **11**, 642-649.

Tsai, J. and Kam, L. (2009). Rigidity-dependent cross talk between integrin and cadherin signaling. *Biophys. J.* **96**, L39-L41.

Tsai, C. C., Huang, R. N., Sung, H. W. and Liang, H. C. (2000). In vitro evaluation of the genotoxicity of a naturally occurring crosslinking agent (genipin) for biologic tissue fixation. *J. Biomed. Mater. Res.* **52**, 58-65.

Vivas-Mejia, P., Benito, J. M., Fernandez, A., Han, H. D., Mangala, L., Rodriguez-Aguayo, C., Chavez-Reyes, A., Lin, Y. G., Carey, M. S., Nick, A. M. et al. (2010). c-Jun-NH2-kinase-1 inhibition leads to antitumor activity in ovarian cancer. *Clin. Cancer Res.* **16**, 184-194.

Weston, C. R., Wong, A., Hall, J. P., Goad, M. E., Flavell, R. A. and Davis, R. J. (2004). The c-Jun NH2-terminal kinase is essential for epidermal growth factor expression during epidermal morphogenesis. *Proc. Natl. Acad. Sci. USA* **101**, 14114-14119.

Wiznerowicz, M. and Trono, D. (2003). Conditional suppression of cellular genes: lentivirus vector-mediated drug-inducible RNA interference. *J. Virol.* **77**, 8957-8961.

Yang, D. D., Conze, D., Whitmarsh, A. J., Barrett, T., Davis, R. J., Rincón, M. and Flavell, R. A. (1998). Differentiation of CD4+ T cells to Th1 cells requires MAP kinase JNK2. *Immunity* **9**, 575-585.

Yang, Y. M., Bost, F., Charbono, W., Dean, N., McKay, R., Rhim, J. S., Depatie, C. and Mercola, D. (2003). C-Jun NH(2)-terminal kinase mediates proliferation and tumor growth of human prostate carcinoma. *Clin. Cancer Res.* **9**, 391-401.

Yeung, T., Georges, P. C., Flanagan, L. A., Marg, B., Ortiz, M., Funaki, M., Zahir, N., Ming, W., Weaver, V. and Janmey, P. A. (2005). Effects of substrate stiffness on cell morphology, cytoskeletal structure, and adhesion. *Cell Motil. Cytoskeleton* **60**, 24-34.

You, H. and Laychock, S. G. (2009). Atrial natriuretic peptide promotes pancreatic islet beta-cell growth and Akt/Foxo1a/cyclin D2 signaling. *Endocrinology* **150**, 5455-5465.

Young, P., Boussadia, O., Halfter, H., Grose, R., Berger, P., Leone, D. P., Robenek, H., Charnay, P., Kemler, R. and Suter, U. (2003). E-cadherin controls adherens junctions in the epidermis and the renewal of hair follicles. *EMBO J.* **22**, 5723-5733.

Yu, C., Minemoto, Y., Zhang, J., Liu, J., Tang, F., Bui, T. N., Xiang, J. and Lin, A. (2004). JNK suppresses apoptosis via phosphorylation of the proapoptotic Bcl-2 family protein BAD. *Mol. Cell* **13**, 329-340.

Zhang, Y. H., Wang, S. Q., Sun, C. R., Wang, M., Wang, B. and Tang, J. W. (2011). Inhibition of JNK1 expression decreases migration and invasion of mouse hepatocellular carcinoma cell line in vitro. *Med. Oncol.* **28**, 966-972.

Journal of Cell Science